Investigation of Transonic Flow Behavior around a Three-Dimensional Turret Using Particle Image Velocimetry

Carlos Caballero

College of Engineering, University of Florida

Light distortions produced by flow density gradients, commonly referred as aero-optic aberrations, remain one of the main sources of laser degradation for airborne laser and other optical systems. At transonic speeds (Ma = 0.7), the flow separation and recirculation regions from highly complex flows around aero-optic housings on aircraft are known to greatly diminish the range and intensity of existing laser systems. Although extensive research has been conducted in the lower subsonic regime, more information is warranted in the transonic regime to better understand the phenomena. The purpose of this investigation is twofold: implement particle image velocimetry (PIV) to corroborate existing research as well as study the flow patterns around the wake region of a hemispherical turret model subjected to transonic flow. PIV is a non intrusive measurement technique where the flow is seeded with small tracer particles. These particles are subsequently illuminated by specialized lasers sheets so that the particle movements can be recorded and the velocity field obtained. By using PIV, an ensemble-average flow velocity map is obtained and can be compared with steady pressure and flow visualization data. The results indicated the emergence of a recirculation region behind the turret model. The shear layer detachment is also readily apparent. However, more research needs to be conducted to ascertain the nature of the recirculation region since seeding the wake was especially challenging.

INTRODUCTION

Airborne laser systems have long been coveted as a potential aircraft systems for many applications because of their zero time of flight and large angular coverage if housed in a turret [1]. Such aero optical aircraft turrets are generally hemispherical and blunt in nature, protruding from the surface as shown in Figure 1 [2]. As a result, flow separation and recirculation regions from highly turbulent shear layers, and potential shocks originating over the aft section of the laser turrets form highly complex flows. These flow phenomena diminish the laser effectiveness by greatly decreasing their range and intensity [1].

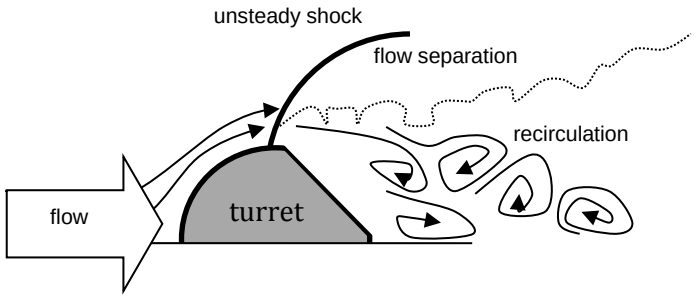

Figure 1. Flow schematic around aero-optical aircraft turret at transonic speeds.

Near field flow effects, or those laser degradations effects created by the flow region immediately surrounding the turret, are referred to as aero-optic aberrations. On the other hand, the laser degradation effects resulting from density and temperature fluctuations in the atmosphere are referred as atmospheric effects [1]. Other sources of degradation are categorized as those related to the laser device and the beam control system, as shown in Figure 2.

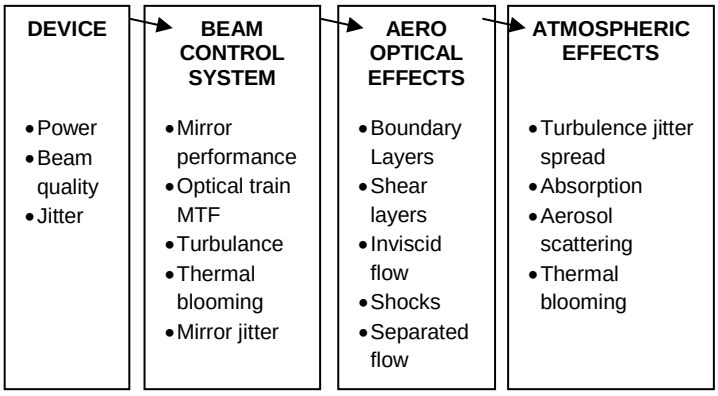

Figure 2. Sources of laser degradation [1].

Recent advances in adaptive optics have compensated for many of these sources of laser degradation, especially those dealing with atmospheric effects [1]. However, aero-optic aberrations remain a significant source of laser degradation that must be addressed [2]. Although extensive research has been conducted in the lower subsonic regime, more information is warranted in the transonic regime, where the density gradients are potentially stronger and linked to the turbulent flow.

In this investigation, Particle Image Velocimetry (PIV) was used to examine the flow around a hemispherical turret at transonic speed (Mach = 0.7) in an effort to better

understand the aero-optic problem in the transonic regime. Before delving into PIV, a physical background on aero-optic aberrations will be introduced. Afterwards, a concise description of the PIV background theory and experimental setup will be described. Finally, the results obtained will be presented and discussed.

Aero-optic Aberrations

Unlike a light bulb which emits light in all directions, a laser emits light in a single direction. This planar wavefront is distorted by flow phenomena that cause density gradients such as shocks, separated flows, and turbulent flows. As light passes through these density gradients, the light is refracted. The laser rays, once perpendicular to the laser wavefront, emerge in different directions, decreasing the laser intensity as shown in Figure 3.

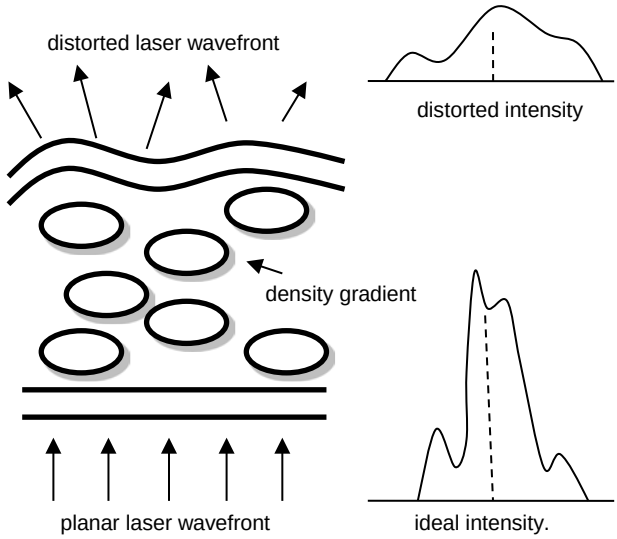

Figure 3. Schematic (not to scale) of aero-optic effect on laser intensity [1][3].

Particle Image Velocimetry

Particle Image Velocimetry is a nonintrusive flow measurement technique with high spatial resolution which relies on illuminated flow particles to obtain flow velocity information. In PIV, the flow is injected (seeded) with small tracer particles (~1 μm in diameter) which are assumed to follow the flow. A specialized laser sheet illuminates the particles around the area of interest in known intervals, allowing the movement of particle groups to be recorded. The resulting images are recorded by cameras, divided into interrogation areas, and used to extract vector fields and a corresponding ensemble-average flow velocity map [4]. The general schematic of a PIV recording technique is shown in Figure 4.

The ensemble-average flow velocity map is a statistical analysis where the velocity vectors in all the recorded velocity fields are averaged. The resulting velocity field

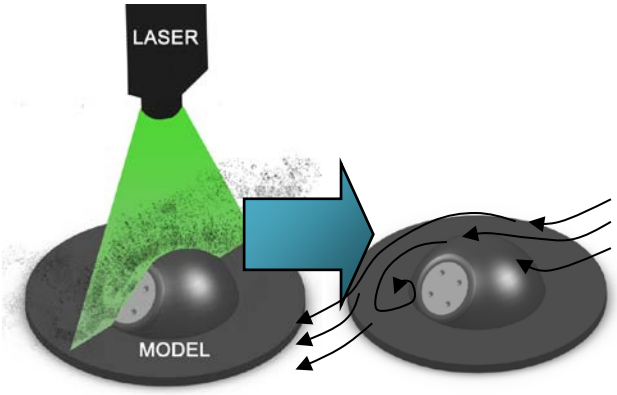

Figure 4. Schematic of piv recording technique.

describes the general flow structures within the flow assuming that the experiments are performed under near identical experimental conditions [5].

Goals

The purpose of this investigation is twofold: to implement particle image velocimetry (PIV) to corroborate existing research (oil flow visualizations, steady pressure measurements) and to study the flow patterns around the wake region of a hemispherical turret model subjected to transonic flow. The oil flow visualization results and steady pressure measurements are presented in Figure 5 and Figure 6 respectively. These results were obtained by fellow researcher Benjamin George in the Transonic Wind Tunnel Facility at the University of Florida and presented here with permission.

In the oil flow visualization experiment, an kerosene-lampblack paint mixture was used to mark the flow streamlines. As the flow passes through the model section, the mixture is sheared and dried, leaving the streamlines that can be analyzed afterwards in a qualitative manner. The oil flow visualization results demonstrated the emergence of stagnation points in front and behind the model. More importantly, the flow appears to detach from the model (separation line) and then form a recirculation region behind the model, next to the optical flat.

The steady pressure measurements involved using an array of pressure taps to measure the pressure distribution throughout the model. The taps were located in a series of columns as shown in Figure 6. Similar to the oil flow visualizations, the steady pressure measurements demonstrated the emergence of a stagnation point in front of the model. The great decrease in the pressure coefficient C_p suggests an increase in flow velocity. Around the apex of the turret (Θ = 120°), the C_p values begin to level out. This trend suggests that the flow has detached from the model due to a high pressure located next to the optical flat. Both the detached shear layer and recirculation region represent unwanted sources of density gradients which need to be minimized.

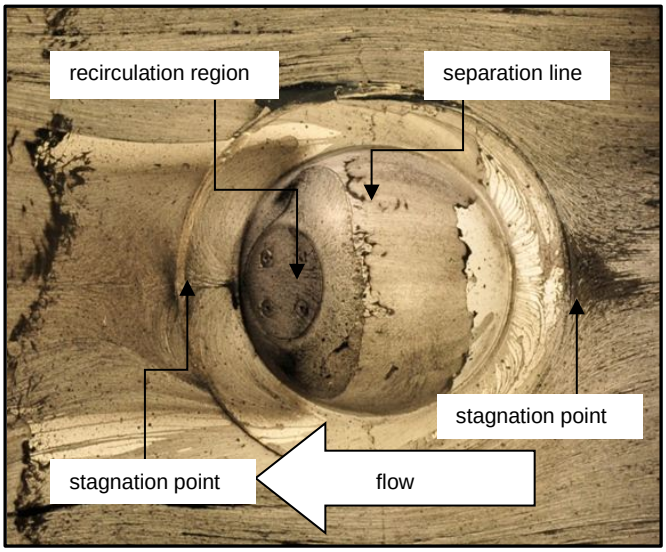

Figure 5. Oil flow visualization results turret courtesy of benjamin george at the university of florida transonic wind tunnel facility. Notice the location of the recirculation region and stagnation points.

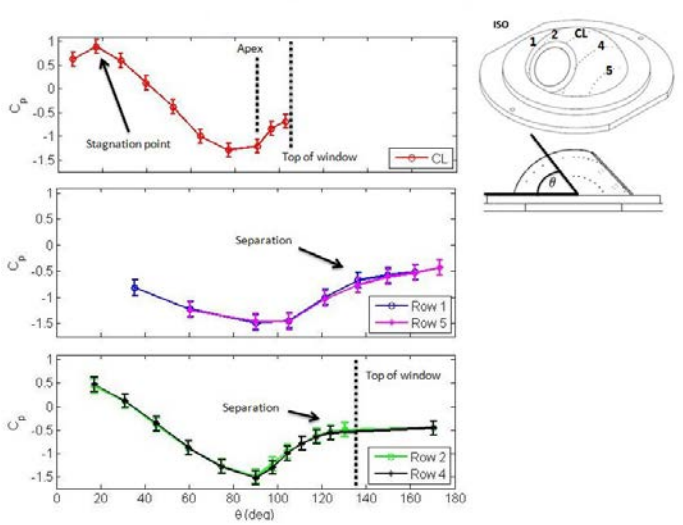

Figure 6. Model steady pressure measurements with respect to ***ɵ*** for (a) the centerline, (b) rows 1 and 5, (c) rows 2 and 4. These results were obtained by benjamin george at the university of florida transonic wind tunnel facility. Notice the location of the stagnation point, separation, and high pressure region.

EXPERIMENTAL SETUP

Turret Model

Figure 7 shows the main characteristics of the turret under investigation. The turret model possesses an optical flat (window) at an angle α = 42° with respect to the vertical. The turret has a height h = 1.1" and a height to radius value (h/R) of 0.771 and a base diameter c = 2.78".

University of Florida Transonic Wind Tunnel

The Transonic Wind Tunnel Facility at the University of Florida is a blowdown wind tunnel configured to reach

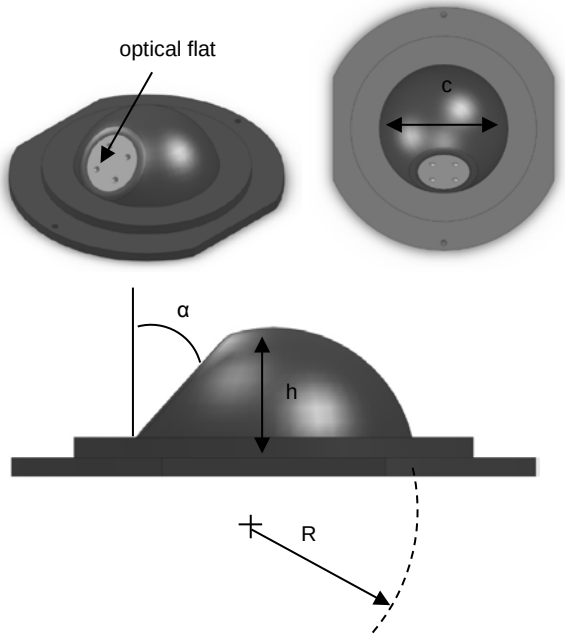

Figure 7. Turret model geometry.

speeds of up to Mach = 0.8. The tunnel test section is 6.5" wide, 6" high, and 14" long. The test section possesses an opening through one of the side walls for mounting the model, as shown in Figure 8. The opposite wall and the top wall of the test section have windows for viewing.

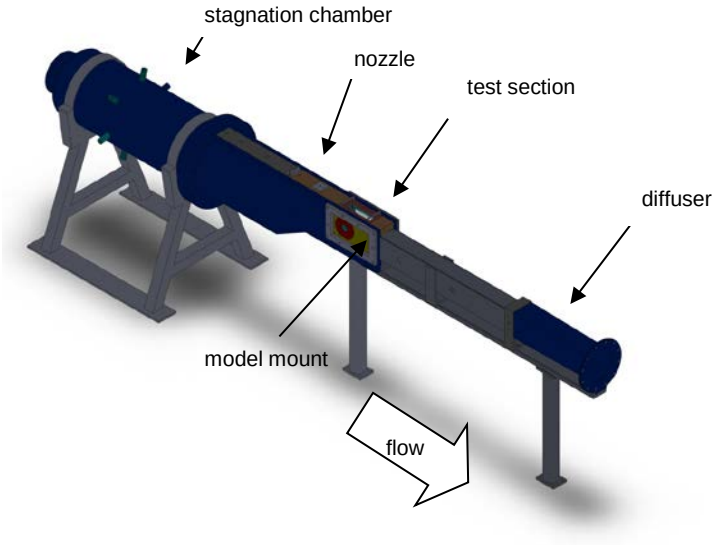

Figure 8. University of Florida transonic wind tunnel.

PIV Setup

The main PIV components include the laser system, the camera, the camera mount and the seeding mechanism. The camera was mounted on top of the tunnel while the laser head was located sideways as shown in Figure 9. In this manner, the laser sheet entered through the tunnel side window and illuminated the model centerline.

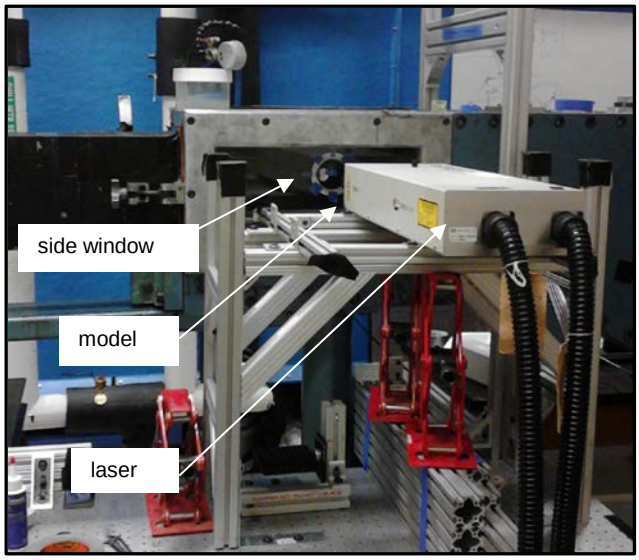

(a)

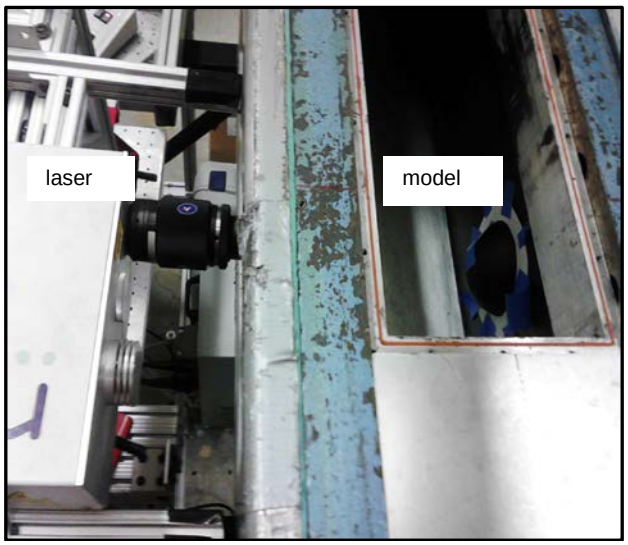

(b)

Figure 9. PIV laser setup showing the position of the laser head with respect to the turret model (a) and close-up view of laser setup (b).

Camera and Laser

A LaVision PIV system consisting of a Litron Nano L 135-15 laser and a pair of Imager ProX-4M cameras were used for this investigation. The laser system creates a pair of 532 nm wavelength pulses at 135 mJ/pulse. The cameras have a nominal resolution of 2048 by 2048 pixels and are capable of recording at 14 frames per second. The camera was set up to view an area of 6 " by 3.5" as shown in Figure 10. The vector field had a resolution of 0.046" between vectors. Due to funding and time constraints, only the centerline was investigated. The centerline was chosen as the area of interest not only because of symmetry but also because the greatest velocity gradients are expected to be located around the centerline.

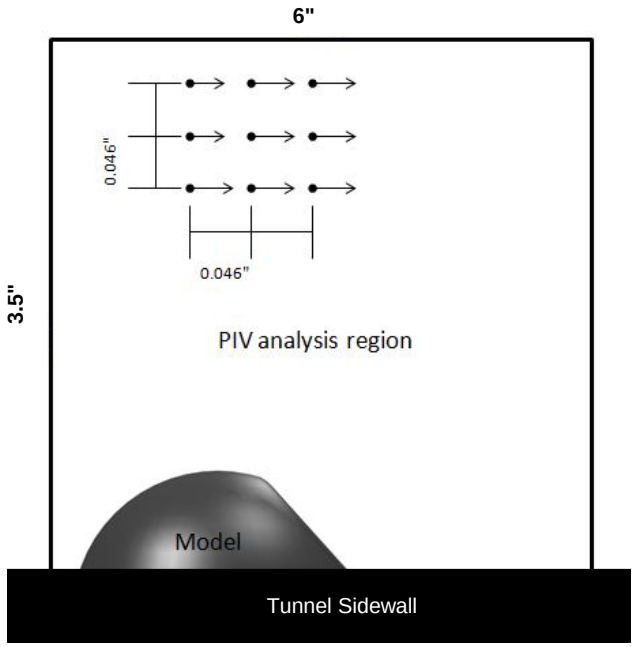

Figure 10. PIV area selection schematic.

Camera Mount

Since the turret model was mounted sideways, the camera was be suspended on top of the tunnel by a traverse as shown in Figure 11. The traverse allowed adjustments in all three directions. The structure was riveted to the floor in order to avoid unwanted vibrations.

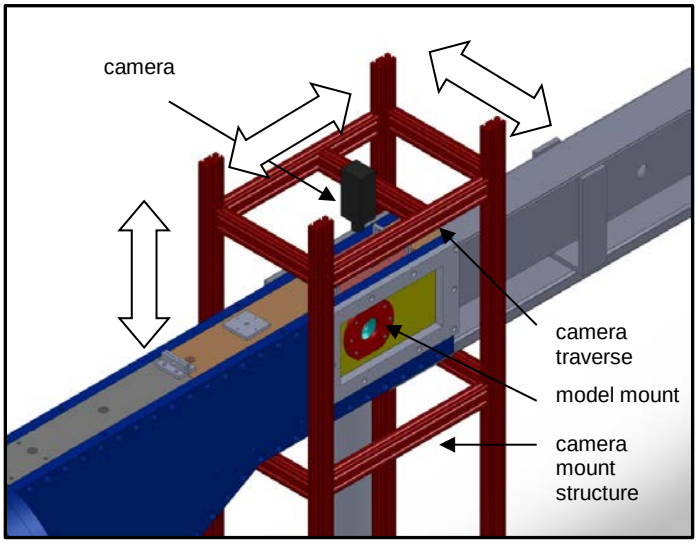

Figure 11: Camera mount structure.

Seeding Mechanism

The seeding mechanism was constructed by connecting dispensing tubes to a LaVision Laskin nozzle. The main dispensing tubes were situated horizontally inside the stagnation chamber. Additional dispensing tubes were arranged in such a way so that the centerline had sufficient

seeding. Olive oil was used for seeding because it is safe, clean, and easy to use.

RESULTS

Normalization

The following section presents the ensemble-average results after processing. The images are normalized with respect to the freestream velocity U_∞ obtained from the definition of Mach number:

$$\boldsymbol{M = \frac{v}{a} = \frac{U_\infty}{a}} \quad (1)$$

where M is the mach number, a is the speed of sound, v is the flow velocity in meters per second. The speed of sound a can be represented as shown in Equation 2 where γ is the ratio of specific heats (1.4 for air), R is the gas constant ($287 \frac{J}{Kg\,K}$ for air), and T_∞ represents the local temperature in kelvin.

$$\boldsymbol{M = \frac{U_\infty}{\sqrt{\gamma R T_\infty}}} \quad (2)$$

Solving for $\boldsymbol{U}_\infty$ and plugging $M = 0.7$ and $T_\infty = 271.1\ K$, the freestream velocity becomes $\boldsymbol{231 \frac{m}{s}}$. The local temperature was in turn obtained using the following isentropic relation:

$$\boldsymbol{\frac{T_\infty}{T_o} = \left(1 + \frac{\gamma - 1}{2} M^2\right)^{-1}} \quad (3)$$

where T_o temperature is the stagnation chamber temperature ($T_o|_{M=0.7} = 297.7\ K$).

Velocity Components

The velocity vectors within each interrogation region can be described with respect to each velocity component in the following manner:

$$\boldsymbol{u = \bar{u} + \underline{u}'} \quad (4)$$

$$\boldsymbol{v = \bar{v} + \underline{v}'} \quad (5)$$

where u corresponds to the horizontal velocity component and v corresponds to the vertical velocity component. The velocity measurements are not identical from measurement to measurement but instead fluctuate around a local mean velocity represented by $\bar{u}$ and $\bar{v}$. A standard deviation is used to describe the amount of fluctuation and is described in Equation 4 and Equation 5 by $\underline{u}'$ and $\underline{v}'$. The standard deviation therefore provides a measure of the turbulence within the flow. The MATLAB functions *nanmean* and *nanstd* were used to obtain the average velocity values and standard deviations within each interrogation region. The *u*-velocity component and the corresponding standard deviation are presented in Figure 12 and Figure 13. The *v*-velocity component and the corresponding standard deviation are shown in Figure 14 and Figure 15 respectively.

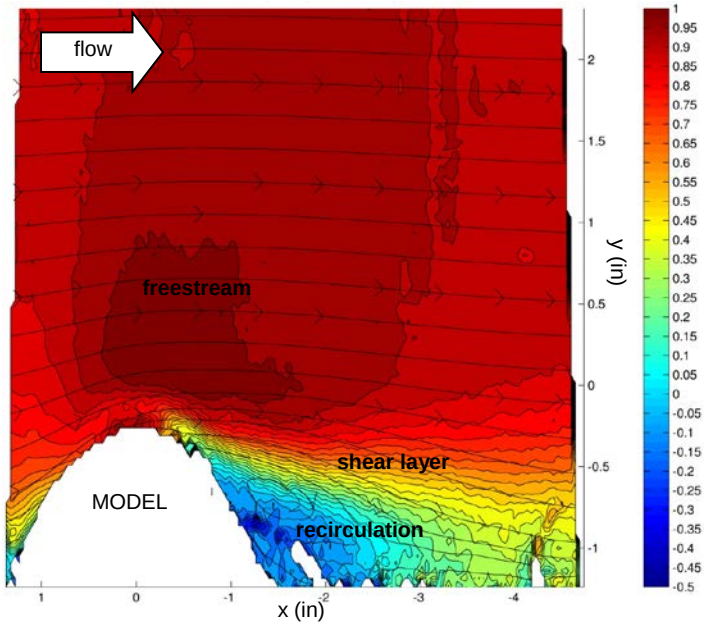

Figure 12. Normalized *u*-component.

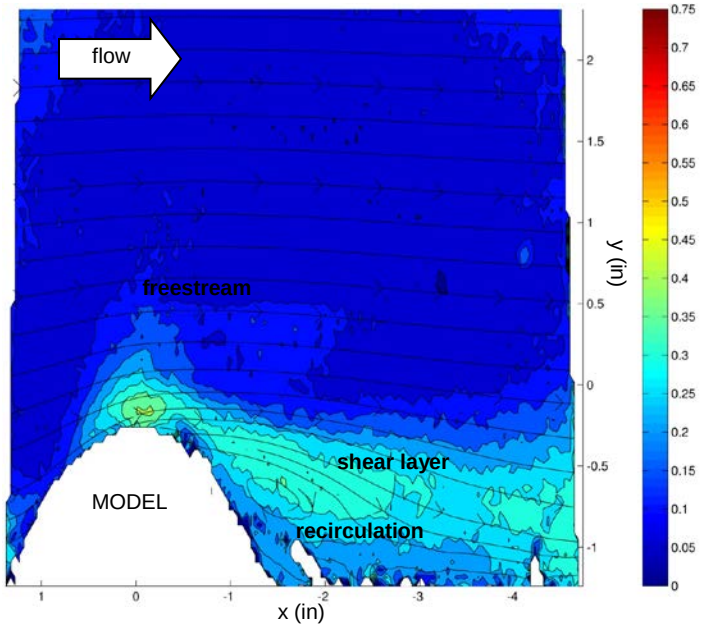

Figure 13. Normalized *u*-component standard deviation.

Number of Vectors

Figure 16 shows the number of vectors used per interrogation region during processing. Even though a total of 827 vector fields were used, the number of available vectors decreased substantially in the wake since the tracer particles tend to follow streamlines. In essence, the seeding particles are pushed away by the high pressure region behind the model, thus preventing them from providing information about the wake region. PIV relies on the presence of these seeding particles to obtain the

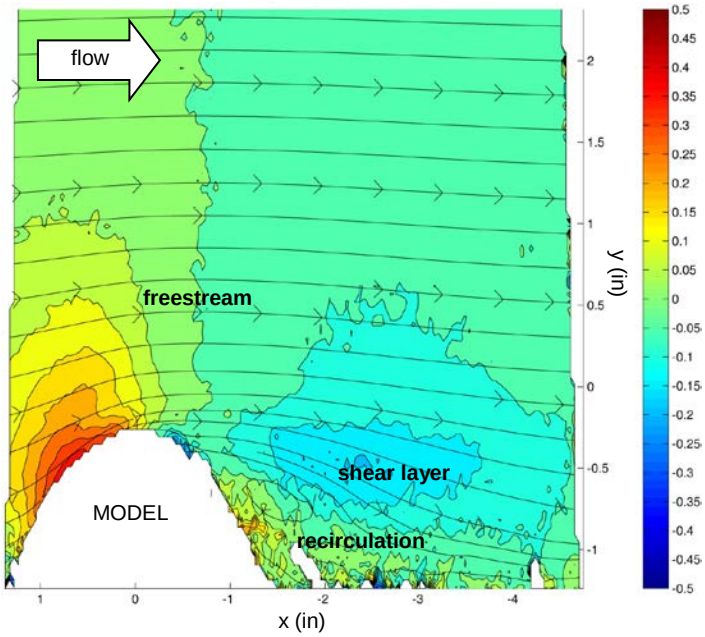

Figure 14. Normalized v-component.

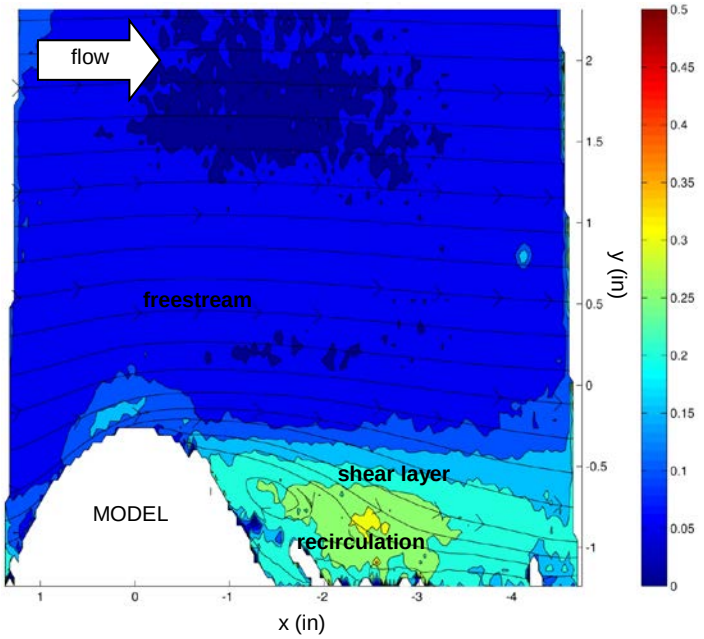

Figure 15. Normalized v-component standard deviation.

local corresponding velocity vector. If no seeding particles are present at the time of recording, no meaningful data can be obtained.

DISCUSSION

As described by Bernoulli's principle, velocity gradients emanate from pressure gradients within a flow. High static pressure regions emerge from low speed flows while low static pressures emanate from high speed flows. As the flow passes over the turret, the flow accelerates since it is being pushed by a high pressure region (stagnation point) in front of the model. The flow eventually encounters a second high pressure region behind the turret model which detaches the flow around the apex of the turret. The flow

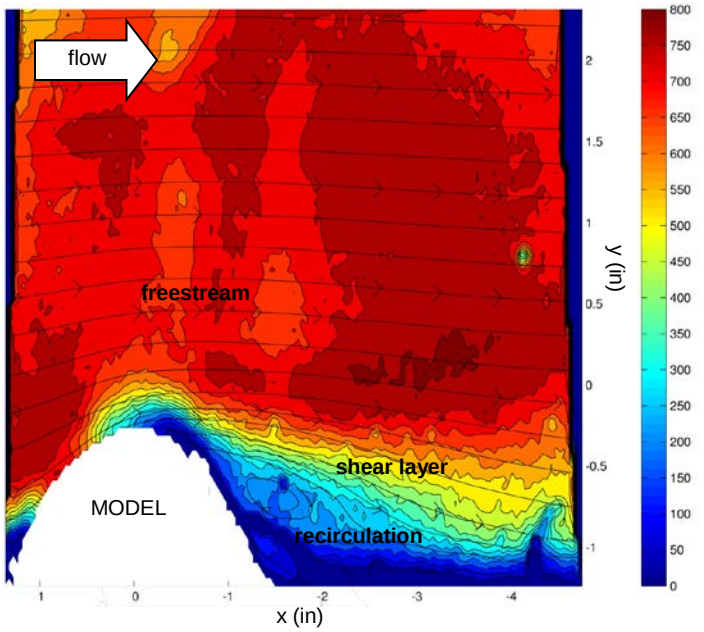

Figure 16. Number of vectors used during processing.

no longer follows the model contour, but is instead pushed away by this region of high pressure/low speed recirculation. The PIV images show the emergence of this recirculation region behind the model having velocities on the order around 15% of freestream velocity.

Such phenomenon was previously demonstrated by the steady pressure measurements and oil flow visualization experiments which indicated the emergence of stagnation points in front and behind the turret, flow acceleration through the model, and separation at the apex of the turret caused by recirculation behind the turret. The streamlines indicate that the recirculation region extends about 0.85*h* behind the window which is consistent with flow visualization experimental results.

The standard deviation of both the horizontal velocity component (*u*-component) and the vertical velocity component (*v*-component) increased around the recirculation and shear layer region, hinting at the turbulent nature of these regions. The *u*-component in the shear layer varied by as much as 35% of local mean velocity while the *v*-component varied by as much as 30%. In comparison, the freestream region which is fairly uniform only had a standard deviation of 5%. The standard deviation was also greatest at the apex of the turret, where the velocities varied as much as 40%. Although shocks might be driving this phenomenon, it is believed that the lack of adequate seeding at the apex of the turret might have played a greater role in generating the enormous velocity variations.

The lack of sufficient seeding in the wake region remains a challenging problem that needs to be addressed. During experimentation, the location of the seeding tubes was adjusted several times to try to take advantage of the wake turbulence to enhance the seeding process. However, no definite location proved ideal.

CONCLUSION

Although the recirculation flow structure is visible in the PIV images, more experiments are required to ascertain the nature of the recirculation region since seeding the flow behind the turret was especially challenging. Indeed, the number of vectors used decreased to practically zero below the shear layer shedding doubt about the accuracy of the velocity results in the wake area. However, the information obtained in this PIV experiment does corroborate some existing data about the nature of the flow around the turret model in the transonic regime. The detachment of the shear layer around the apex of the turret is readily apparent. Flow acceleration through the model before shear detachment is also apparent, corroborating the steady pressure measurements. The *u*-component in the shear fluctuated by 35% while the *v*-component fluctuated by as much as 30%, compared to only 5% in the freestream region hinting at the turbulent nature of the wake area.

Only the model centerline was investigated in this analysis. Therefore, any future work should try to explore other areas around the centerline, incorporating other PIV methods better suited for 3D flows such as stereoscopic PIV. Finally, special attention should be given to seeding. Finding a way to reliably seed the wake and recirculation region is imperative for obtaining meaningful data about the flow in these regions.

ACKNOWLEDGEMENTS

I want to thank Dr. Lawrence Ukeiley for his dedicated support, giving me the tools to push this project forward. I also want to thank Benjamin George and Kyle Hughes for their immense assistance in preparing, conducting, and analyzing the experiments and experimental results. Special thanks to other members of the Interdisciplinary Microsystems Group (IMG) for contributing in some way or another and giving me the advice and know how about PIV. To all of you, thank you

REFERENCES

[1] K. G. Gilbert and L. Otten, "Aero-optical phenomena," *American Institute of Aeronautics and Astronautics*, vol. 80, 1982.

[2] M. Palaviccini, "Control of three-dimensional flow over a turret," University of Florida, 2011.

[3] E. J. Jumper and E. J. Fitzgerald, "Recent advances in aero-optics," *Progress in Aerospace Sciences*, vol. 37, no. 3, pp. 299–339, Apr. 2001.

[4] M. Raffel, C. Willert, S. Wereley, and J. Kompenhans, *Particle Image Velocimetry: A Practical Guide*. New York: Springer, 2007.

[5] R. J. Adrian and J. Westerweel, *Particle Image Velocimetry*. New York: Cambridge University Press, 2011.